Chemical Engineering Science 100 (2013) 352–359

Contents lists available at SciVerse ScienceDirect

Chemical Engineering Science

journal homepage: www.elsevier.com/locate/ces

Process intensification and optimization for hydroxyapatite nanoparticles production

Filipa Castro [a,*], Simon Kuhn [b], Klavs Jensen [c], António Ferreira [a], Fernando Rocha [d], António Vicente [a], José António Teixeira [a]

[a] IBB—Institute for Biotechnology and Bioengineering, Centre for Biological Engineering, University of Minho, Campus de Gualtar, 4710-057 Braga, Portugal
[b] Department of Chemical Engineering, University College London, Torrington Place, London WC1E 7JE, United Kingdom
[c] Department of Chemical Engineering, Massachusetts Institute of Technology, 77 Massachusetts Avenue, Building 66-350, Cambridge, MA 02139-4307, United States of America
[d] LEPAE—Laboratory for Process, Environmental and Energy Engineering, Faculty of Engineering of the University of Porto, Rua Roberto Frias, s/n, 4200-465 Porto, Portugal

HIGHLIGHTS

- An ultrasonic tubular microreactor was studied for the synthesis of HAp.
- HAp was synthesized by continuous precipitation from solution.
- Single-phase flow and gas–liquid flow were both investigated.
- HAp was produced under near-physiological conditions of temperature and pH.
- HAp particles show improved quality compared to commercial powder or batch synthesis.

ARTICLE INFO

Article history:
Received 31 August 2012
Received in revised form
14 December 2012
Accepted 2 January 2013
Available online 9 January 2013

Keywords:
Hydroxyapatite
Microreactor
Precipitation
Laminar flow
Segmented flow
Aggregation

ABSTRACT

Precipitation processes are widely used in industry for the production of particulate solids. Efficient mixing of the reagents is of major importance for the chemical and physical nature of the synthesized particles. Recently, microreactors have been studied to overcome homogeneity problems found when using stirred tank batch reactors. The present work investigated an ultrasonic tubular microreactor for the continuous-flow precipitation of hydroxyapatite (HAp), both in single-phase flow (SPF) and in gas–liquid flow (GLF). HAp nanoparticles were yielded for both configurations under near-physiological conditions of pH and temperature. The as-prepared particles, especially those that were prepared under GLF, show improved characteristics compared to commercial powder or powder obtained in a stirred tank batch reactor. Primary particles are smaller, particle shape is more homogeneous, and the aggregation degree of the particles is lower.

1. Introduction

The synthesis of powders with controlled shape and narrow particle size distribution continues to be a central challenge in chemical industry. Among all the methods for producing particles, wet chemical synthesis in stirred tank batch reactors is the most interesting route because of its simplicity, low cost, and easy application in industrial production (Kawase and Miura, 2007; Liu et al., 2001; Ying et al., 2008).

In classic colloidal chemistry, the particle formation goes through three stages in the liquid phase, i.e., nucleation, growth companying with Ostwald ripening, and aggregation. During reactive precipitation, high levels of supersaturation are generated, leading to rapid nucleation and growth of solid phases. Therefore, mixing effects are significant in determining the distribution of supersaturation and subsequently the particle size distribution of the product. Due to the insufficient mixing in stirred tank batch reactors, the nonuniform distribution of the nuclei and different residence times of growth and aggregation occur, yielding particles with broad size distribution (Chen et al., 1996; Mersmann, 1999; Trippa and Jachuck, 2003; Ying et al., 2008). The problem becomes magnified as the scale of operation increases (Jones et al., 2005).

* Corresponding author. Tel.: +351 253 604400; fax: +351 253 678986.
E-mail address: fcastro@deb.uminho.pt (F. Castro).

0009-2509/$ - see front matter © 2013 Elsevier Ltd. All rights reserved.
http://dx.doi.org/10.1016/j.ces.2013.01.002

The use of tubular microreactors seems to be a promising way to solve a lot of limitations related to stirred tank batch reactors. Transfer processes, mixing of reactants as well as residence time are very fast in microstructured devices, allowing a better control over the reaction conditions (Hung and Lee, 2007; Jähnisch et al., 2004; Kockmann et al., 2008; Song et al., 2008). Further, microreactors have the ability to operate within continuous flow regimes (Hartman and Jensen, 2009), which besides being more productive and able to promote more homogeneous reaction conditions, yet permits the continuous variation of the chemical composition of the reaction medium (Song et al., 2008; Zhao et al., 2011).

However, particle processing in microchannels presents difficulties due to parabolic flow and channel clogging (Kockmann et al., 2008). In this context, segmented-flow microreactors have been investigated, since they can narrow the residence time distribution and generate uniform particles of narrow size distribution (Gunther and Jensen, 2006). As to channel clogging, it is mainly caused by wall attachment of particles and by particle aggregation. In the first case, an accurate choice of the tube material and/or coating of the wall can solve the problem. In the case of particle aggregation, it can be significantly reduced by the use of ultrasound, as shock waves created by cavitation can shorten the contact time between particles and prevent their bonding together (Luque de Castro and Priego-Capote, 2007).

Hydroxyapatite $Ca_5(PO_4)_3OH$ (HAp) is widely used as bone substitute material due to its exceptional biocompatibility, bioactivity and osteoconductivity (He and Huang, 2007). As these properties are directly related to HAp particles characteristics (size, morphology and purity), a very good control of the reaction conditions is required to obtain particles that meet specific requirements, such as high specific surface area (favoured by small crystal sizes), narrow size distribution and high purity.

In the present work, continuous-flow precipitation of HAp was carried out in a tubular microreactor immersed in an ultrasonic bath, where single-phase (laminar) flow and gas–liquid (segmented) flow experiments were both performed. By this way, it is intended to intensify the HAp precipitation process by taking advantage of the dimensions of microreactors, which namely provide intense mixing. Besides, application of ultrasound and especially segmentation of the flow, in addition to facilitating the handling of particles in the microchannels, improve the monodispersity of the particle synthetized. As to the operating conditions, namely temperature, reactants concentration and mixing Ca/P molar ratio, were defined in order to promote spontaneous formation of HAp under near-physiological conditions of temperature (37 °C) and pH (7). Besides HAp being the most stable calcium phosphate at human body temperature and pH, there is a concern in preparing HAp under conditions that are more conductive to the survival of bone related cells. The preparation has to follow specific criteria, namely about pH and temperature conditions (Kumta et al., 2005).

2. Experimental procedure

2.1. Description of the ultrasonic tubular microreactor

Continuous-flow precipitation of HAp was carried out in a tubular microreactor (Fig. 1a) immersed in an ultrasonic bath, where single-phase flow (SPF) and gas–liquid flow (GLF) studies were both performed. As it is exemplified in Fig. 1a, the reactor is constituted by two main parts: a mixing chamber (Upchurch Scientific), with two different configurations depending on the flow type, a T-mixer for SPF and a cross-mixer for GLF; and the tubular reactor (Teflon PFA, Upchurch Scientific) itself of 600 μL,

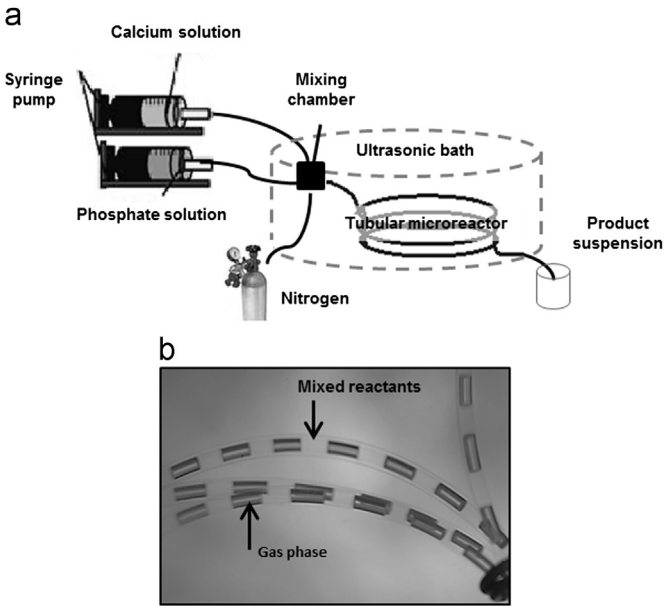

Fig. 1. (a) Schematic representation of the experimental apparatus and (b) picture of a section of the GLF tubular microreactor.

that consists of a spiral tube with 1.02 mm in inner diameter and 1.59 mm in external diameter. The function of the first part of the reactor is to mix thoroughly the reactants and in the case of the GLF its function is also to segment the liquid mixture. The reaction progresses in the second part of the reactor. The segmented gas is used to separate the liquid phase in small entities (Fig. 1b). By this way, the gas phase induces recirculation and enhances mixing within individual liquid slugs. The result is a narrow residence time distribution and reduced particle size polydispersity (Gunther and Jensen, 2006; Song et al., 2008).

The reactants were fed into the set-up by means of a syringe pump (Harvard PHD 2000) and kept at 37 °C through the use of thermal jackets (McMaster-Carr). With regard to the gas phase, the flow rate of nitrogen was adjusted by a mass flow controller (Sierra FlowBox). The microfluidic connections were provided by Teflon tubing (Upchurch Scientific) with 1.02 mm in inner diameter. The reactor was immersed in an ultrasonic bath (VWR model 50HT, frequency of 40 kHz and power input of 4–8 W) to minimize the potential for clogging the reactor and to enhance mixing. The application of ultrasound produces stable cavitation by degassing the solvent (Mason, 1964). The so generated pressure waves cause the particles to collide into one another with great force, promoting faster nucleation and aggregates breakage (Luque de Castro and Priego-Capote, 2007). Therefore, the use of ultrasound provides a non-invasive (no added chemicals or additional mechanical treatment) way of improving crystal properties and process control. The experiments were started with a temperature of 37 °C in the ultrasonic bath.

2.2. Powder preparation

HAp was synthesized by the mixing of a calcium hydroxide (Sigma-Aldrich, 95%) aqueous solution (0.01926 M) and an orthophosphoric acid (Mallinckrodt, 85%) aqueous solution (0.01448 M) at 37 °C, with a mixing molar ratio Ca/P=1.33. To facilitate the dissolution of calcium hydroxide, the solution was previously agitated for 24 h at 500 rpm, and at 25 °C, as its solubility decreases with temperature (Johannsen and Rademacher, 1999). Both reactants were prepared with ultra-pure water (Milli Q water, resistivity of 18.2 MΩ/cm at 25 °C) and ionic force was adjusted by the

addition of 6 mL of potassium chloride (Mallinckrodt, 99.8%) 4 M solution. Then, both reactants were heated and kept at 37 °C. The operating conditions used are presented in Table 1.

Temperature (J-KEM Scientific) and pH (needle-like tip micro pH electrode, Thermo Fisher Scientific ORION) were continuously measured at different time intervals at the outlet of the microsystem. The pH electrode was calibrated with two buffer solutions with pH=7 and pH=10 at 25 °C. The average pH was close to 7 for all the operating conditions. As to the temperature, values oscillated around 37 °C, since the continuous use of ultrasounds caused a slight increase of it, particularly for the larger residence times. All the experiments were thus conducted under near-physiological conditions of temperature and pH, which is particularly important for the preparation of HAp powders for medical applications (Kumta et al., 2005). Moreover, HAp is thermodynamically the most stable calcium phosphate at human body temperature and pH between 4 and 12 (Elliot, 1994).

Results obtained in our previous work (Castro et al., 2012), where HAp precipitation was conducted in a 1 L stirred tank batch reactor under the same conditions of reagents concentration, mixing Ca/P molar ratio and temperature, will be used for comparison.

Table 1
Operating conditions.

Sample	Flow type	Liquid flow rate (mL/min)	Gas flow rate (standard mL/min)	Liquid residence time τ (min)
SPF 1	Single-phase flow	0.152	–	3.94
SPF 2		0.304	–	1.97
SPF 3		0.608	–	0.99
SPF 4		2.0	–	0.30
SPF 5		4.0	–	0.15
GLF 1	Gas-liquid flow	0.152	1.2	0.43
GLF 2		0.304	1.2	0.39
GLF 3		0.608	1.2	0.34
GLF 4		2.0	1.2	0.19
GLF 5		2.0	2.0	0.15
GLF 6		4.0	1.2	0.12
GLF 7		4.0	4.0	0.08
Batch	–	–	–	330

2.3. Powder characterization

Samples were withdrawn at the outlet of the microreactor, centrifuged (at 1500 rpm for 5 min), washed twice with ultrapure water and conserved in ethanol (Koptec 200 proof pure), which stops the solid–liquid reaction (Bernard et al., 2000). For X-ray diffraction (XRD) (PanAlytical X'Pert PRO MPD) and scanning electron microscopy (SEM) (FEI Quanta 400FEG ESEM/EDAX Genesis X4M, with an accelerating voltage of 20 kV) studies, suspensions were dried at T=80 °C for 24 h. As to SEM analysis, samples were covered by a 10 nm gold layer. For FTIR spectroscopy (Bruker Vertex 70 with MCT detector), a small drop of the suspension was put on a 1 mm thick ZnSe support, dried (80 °C) to evaporate the ethanol and then analyzed. Finally, for particle size distribution analysis, suspensions were collected at the end of each experiment and directly analyzed using a Malvern Mastersizer 2000 apparatus.

3. Results and discussion

3.1. Powder synthesis

3.1.1. Phase identification

XRD patterns of the as-prepared particles are shown in Figs. 2 and 4. Further, Figs. 3 and 5 show magnified XRD patterns of the dominant peaks. In general, all the diffraction patterns show characteristic peaks of HAp (JCPDS 9-0432), though GLF 2 pattern also exhibits peaks assigned to dicalcium phosphate dihydrate (DCPD) (JCPDS 9-77) and to beta-tricalcium phosphate (β-TCP) (JCPDS 9-169) (Figs. 4 and 5). One of the main differences between XRD patterns of the products formed and XRD pattern of a commercial HAp (Spectrum, minimum 40 meshes) is the presence of broader peaks. This suggests the presence of amorphous phases or considerably small size particles (Siddharthan et al., 2005; Victoria and Gnanam, 2002). Further, diffraction patterns show sharp and high intensity peaks at 28° 2θ and 40.5° 2θ, unlike the commercial HAp pattern. Such peaks are characteristic of high crystallinity and large grain size and their position suggests that they are assigned to potassium chloride, used to adjust the ionic strength. This may be explained by the occlusion of KCl. Indeed, part of the mother liquor could have been trapped between the aggregates, and the KCl contained

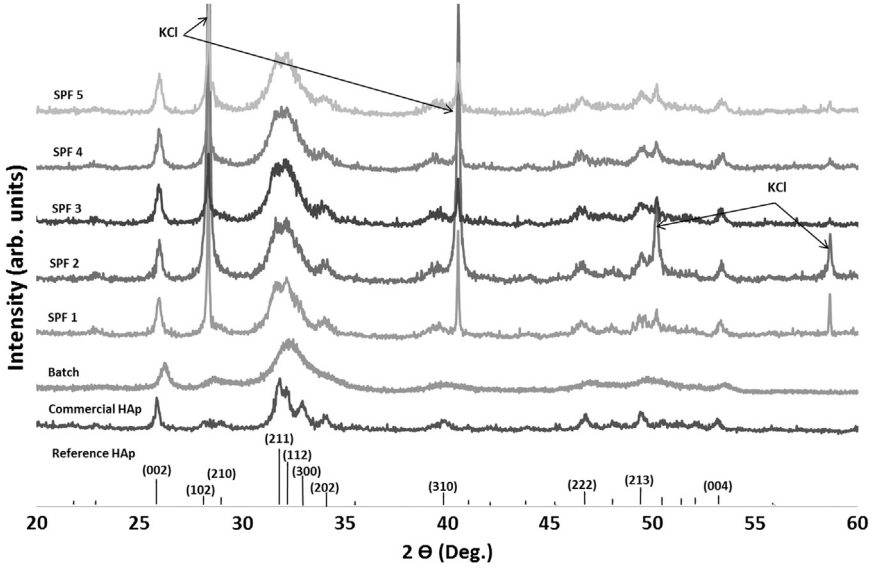

Fig. 2. XRD patterns of the particles produced in the ultrasonic SPF tubular microreactor and in the stirred tank batch reactor.

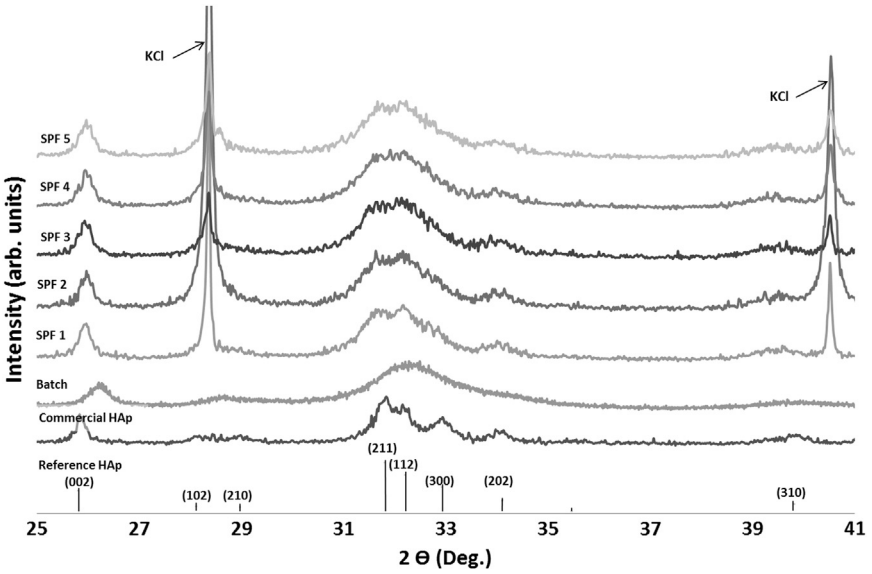

Fig. 3. Magnified XRD patterns of the particles produced in the ultrasonic SPF tubular microreactor.

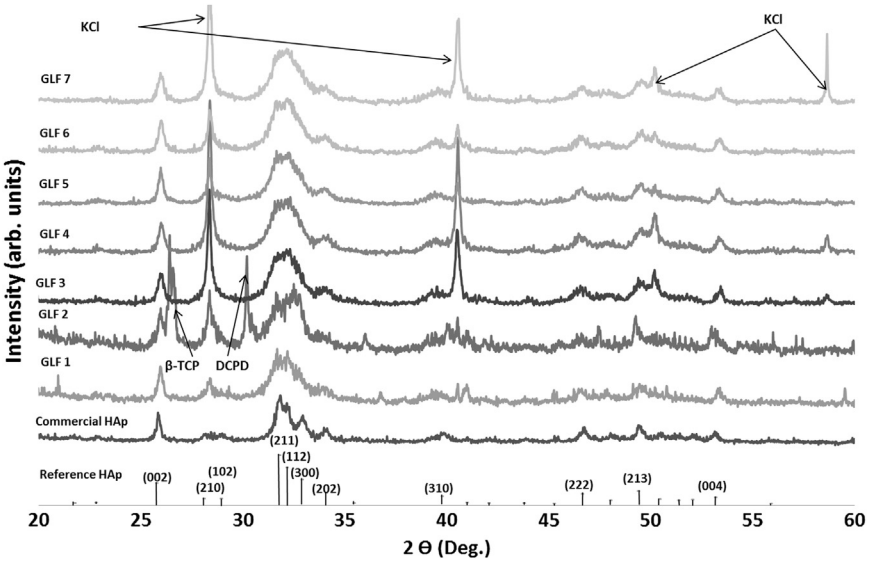

Fig. 4. XRD patterns of the particles produced in the ultrasonic GLF tubular microreactor and in the stirred tank batch reactor.

in the mother liquor crystallized at the drying step. As to the differences between XRD patterns of the samples obtained under laminar flow (Fig. 3), there is no major influence of the residence time on the patterns of the powders obtained. In relation to powders prepared under segmented-flow (Fig. 5), there is no major difference between the precipitates GLF 1, GLF 3, GLF 4, GLF 5, GLF 6 and GLF 7, prepared under different residence times. According to Fig. 5, the only difference between the XRD patterns of those samples is due to the presence of KCL peaks, which in some cases are barely detected. This may be explained by the formation of less aggregated particles that facilitated the removal of the mother liquor during the washing step. As to sample GLF 2, as mentioned above, peaks assigned to other calcium phosphates, namely β-TCP and DCPD were detected. Despite HAp being thermodynamically the most stable calcium phosphate at the existing conditions, other calcium phosphates grow faster and therefore may appear. In these conditions the kinetic factors can assume a decisive role and may thus explain the formation of other calcium phosphates.

FTIR spectra of the as-prepared particles are given in Figs. 6 and 7. All the spectra exhibit the stretching and bending vibrations of the phosphate, PO_4^{3-}, and the hydroxyl, OH^-, functional groups, characteristic of a typical apatite structure (Koutsopoulos, 2002). The peak at 603 cm^{-1} indicates the presence of a $\boldsymbol{\nu_4}$ PO_4^{3-} bending mode. The strong broad band around 1037 cm^{-1} confirms the presence of the $\boldsymbol{\nu_3}$ PO_4^{3-} mode. The sharp peaks at 630 and 3571 cm^{-1} belong to the stretching vibrations of the hydroxyl group. The presence of adsorbed water in the products formed is also verified, as a broad band from approximately 3700 to 3000 cm^{-1} and a peak at 1643 cm^{-1} are observed (Koutsopoulos, 2002; Zhou et al., 2008). This may be justified by the low drying temperature (80 °C) and the absence of a ripening (ageing) treatment (Osaka et al., 1991). The small band around 875 cm^{-1} can be attributed to the vibrational frequencies of carbonate ions or HPO_4^{2-} group (Koutsopoulos, 2002), which is consistent with a carbonated HAp or calcium-deficient HAp. In some cases, spectra show a doublet at 1454 and 1428 cm^{-1} that confirms the CO_3^{2-} carbonate mode of vibration. The

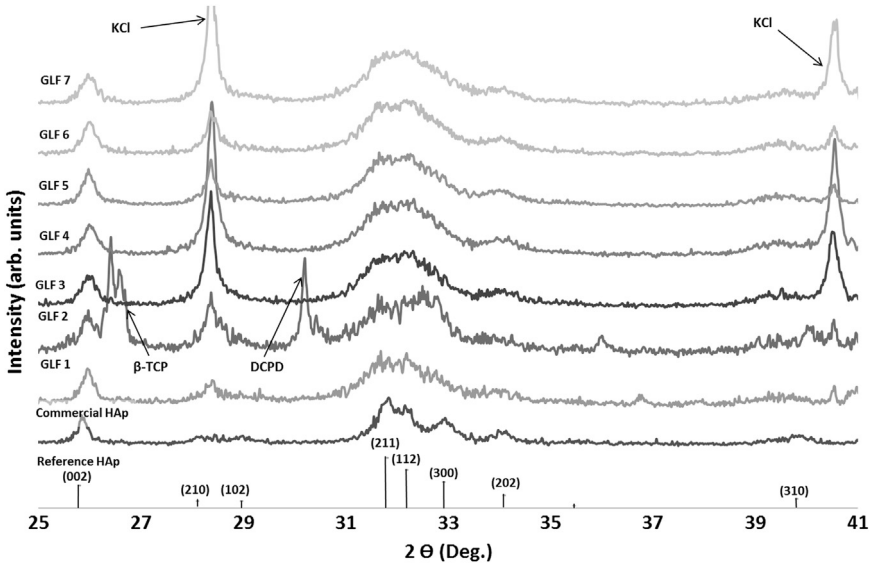

Fig. 5. Magnified XRD patterns of the particles produced in the ultrasonic GLF tubular microreactor and in the stirred tank batch reactor.

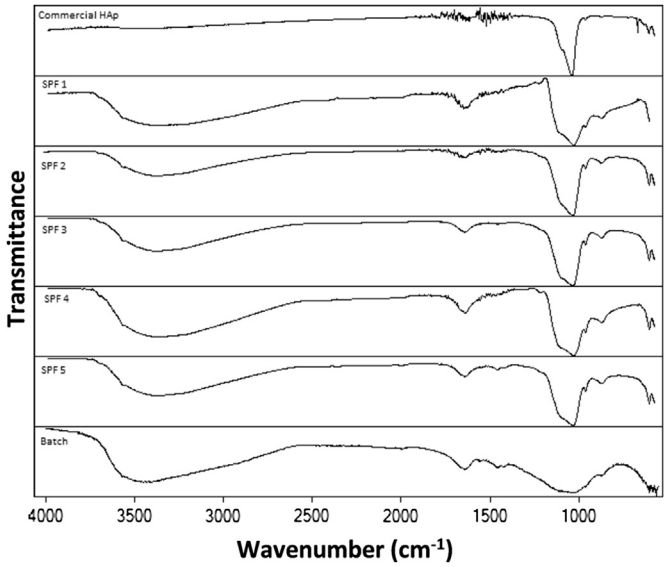

Fig. 6. FTIR spectra of the particles produced in the ultrasonic SPF tubular microreactor and in the stirred tank batch reactor.

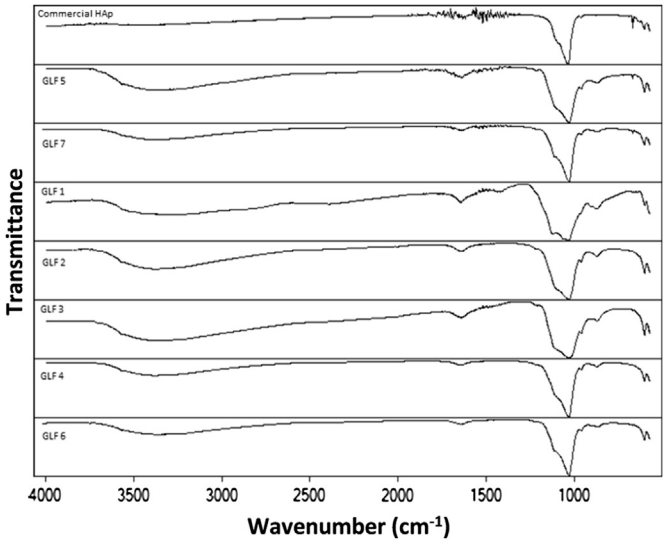

Fig. 7. FTIR spectra of the particles produced in the ultrasonic GLF tubular microreactor.

presence of these bands is characteristic of a carbonated HAp of B-type, where the carbonate ions occupy the phosphate ions sites (Koutsopoulos, 2002; Landi et al., 2003). The presence of carbonate ions can be explained by the absorption of CO_2 from water.

3.1.2. Particle size, particle morphology and particle size distribution

From Fig. 8, the powders prepared consist of nanometric-sized particles and seem to have a rod-like shape. The as-prepared powders were compared to a commercial HAp powder (Spectrum, minimum 40 meshes), originally submitted to granulometric separation. Both commercial and the as-prepared powders present a certain degree of aggregation (Table 2, Figs. 8 and 9). This phenomenon can be justified by the amorphous nature of the particles and their small size, since they possess a high surface area to volume ratio, resulting in a high surface tension, which they tend to lower by adhering to one another (Luque de Castro and Priego-Capote, 2007). Moreover, primary particles are more easily seen for the powders prepared in the GLF tubular microreactor (Fig. 8, GLF 4 and GLF 5), when compared to commercial HAp particles and particles prepared in the SPF tubular microreactor (SPF 4). Particles produced under segmented flow seem to have a more defined shape, while particles produced under laminar flow seem to be more amorphous (Fig. 8) and hence have higher tendency to form aggregates. Indeed, using gas to create a segmented flow results in the formation of small reacting entities separated from each other by gas bubbles, which reduces particle-to-particle interactions, and thus the formation of aggregates (Kuhn et al., 2011). Besides, the introduction of the gas phase creates recirculation and thus enhances mixing within the individual liquid slugs. This leads to a narrow residence time and reduced axial dispersion, resulting thereby in a high degree of supersaturation and a more homogeneous medium, favoring the formation of small and uniform particles (Gunther and Jensen, 2006; Mersmann, 1999; Wang et al., 2007).

As to particle size distribution, for both segmented and laminar flow, one obtains a bimodal distribution, and in some cases trimodal distribution, except for powder SPF 4 (Fig. 9 and

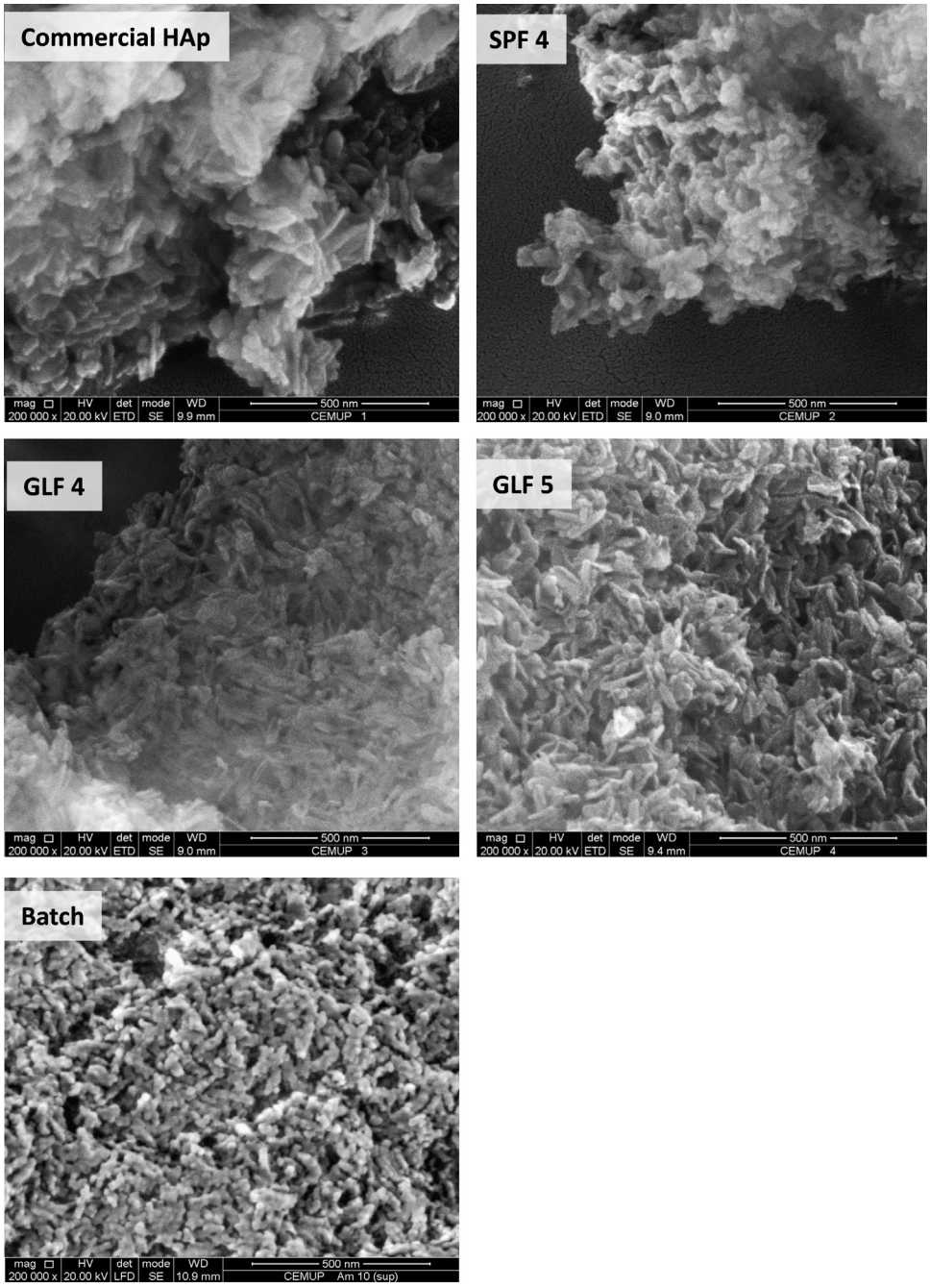

Fig. 8. SEM images of the particles produced in the different reactors studied.

Table 2). The as-prepared powders consist of a population of primary particles in the nanometer range and a population of micrometric-sized aggregates that given the considerable difference in size, could be separated. When compared to the commercial HAp particles, the as-prepared particles possess smaller primary particles (Fig. 9). It is also important to underline that particles produced were directly obtained from the system without thermal treatment and without granulometric separation. In the case of powders produced in the SPF tubular microreactor, one observes that as the residence time decreases the aggregation phenomenon is more pronounced, except for the lower residence time (Fig. 9). It would be expected to obtain smaller particles for higher liquid flow rates, since Reynolds number are higher and mixture efficiency enhanced. This results in a higher supersaturation, which in turn results in rapid nucleation and growth, leading to small particles (Mersmann, 1999; Yang et al., 2009; Ying et al., 2008). However, smaller particles are more susceptible to aggregation at the same conditions, namely at the same ionic strength and pH conditions (He et al., 2008). In this case, smaller particles may have formed as the liquid flow rate increases, but later aggregate given their small size. Regarding the segmentation of the flow, the results show a larger primary particles population, when compared to the powders formed in SPF (Fig. 9 and Table 2). Analyzing parameters of the particle size distribution (Table 2), one can see that d_{10} and d_{50} decrease with segmentation of the flow, approximating to the particle size distribution of the commercial HAp. A third population appears in some cases, consisting in large aggregates of about 200 μm, probably because primary particles are smaller and thus have higher tendency to aggregate.

Table 2
Parameters of the particle size distribution of the powders produced in the different reactors studied. d_{10}: 10% of the particles are smaller than this value, d_{50}: 50% of the particles are smaller than this value; d_{90}: 90% of the particles are smaller than this value; $d_{(4,3)}$ equivalent volume mean diameter; span: width of the distribution based on the 10%, 50% and 90% quantile.

Sample	Particles size (μm)				Span
	d_{10}	d_{50}	d_{90}	$d_{(4,3)}$	
SPF 1	0.15	1.24	43.42	22.06	34.90
SPF 2	0.14	16.96	54.20	23.06	3.19
SPF 3	0.60	32.29	62.83	34.55	1.93
SPF 4	22.59	38.30	62.70	40.90	1.05
SPF 5	0.08	0.25	38.97	17.45	155.56
GLF 1	0.09	0.42	44.56	17.63	105.88
GLF 2	0.13	12.23	53.00	23.74	4.32
GLF 3	0.15	10.35	44.23	19.87	4.26
GLF 4	0.14	13.90	40.94	16.28	3.96
GLF 5	0.13	14.88	52.33	26.18	3.51
GLF 6	0.09	0.35	87.26	24.98	249.06
GLF 7	0.11	10.76	37.67	14.25	3.49
Batch	15.48	36.22	68.11	39.47	1.45
Commercial HAp	0.15	0.59	2.44	1.31	3.88

3.2. Comparison between HAp particles prepared in the ultrasonic tubular microreactor and in the stirred tank batch reactor

Particles synthetized in the stirred tank batch reactor appear to be less crystalline than the particles formed in the ultrasonic tubular microreactor, since its XRD pattern and its FTIR spectrum exhibit broader peaks when compared to XRD patterns and FTIR spectra of the powders prepared in the microreactor (Figs. 2–5). Carbonate contamination seems to be minimized in the microreactors, as carbonate bands at approximately 1454 and 1428 cm^{-1} are clearly exhibited in the spectrum of the HAp powder prepared in the stirred tank batch reactor and in most cases are not present in the spectra of the powders obtained in the microsystems (Figs. 4 and 5). Indeed, systems were not open to air and carbonate ions could only come from the water used in the preparation of the reagents.

Regarding particle size distribution of the powder formed in the stirred tank batch reactor (Fig. 9), micrometric-sized aggregates with a mean size of about 36 μm were observed. Unlike powders prepared in the ultrasonic tubular microreactor, where primary particles in the nanometer range where observed, HAp produced in the stirred tank batch reactor only consists of micrometric-sized aggregates. Due to the high surface-area-to-volume ratio, heat and mass transfer distances are significantly reduced in the tubular microreactor, when compared to the stirred tank batch reactor. These results in a rapid and intense mixing, which, as mentioned above, results in rapid nucleation and growth, leading to the formation of small particles (Wang et al., 2009).

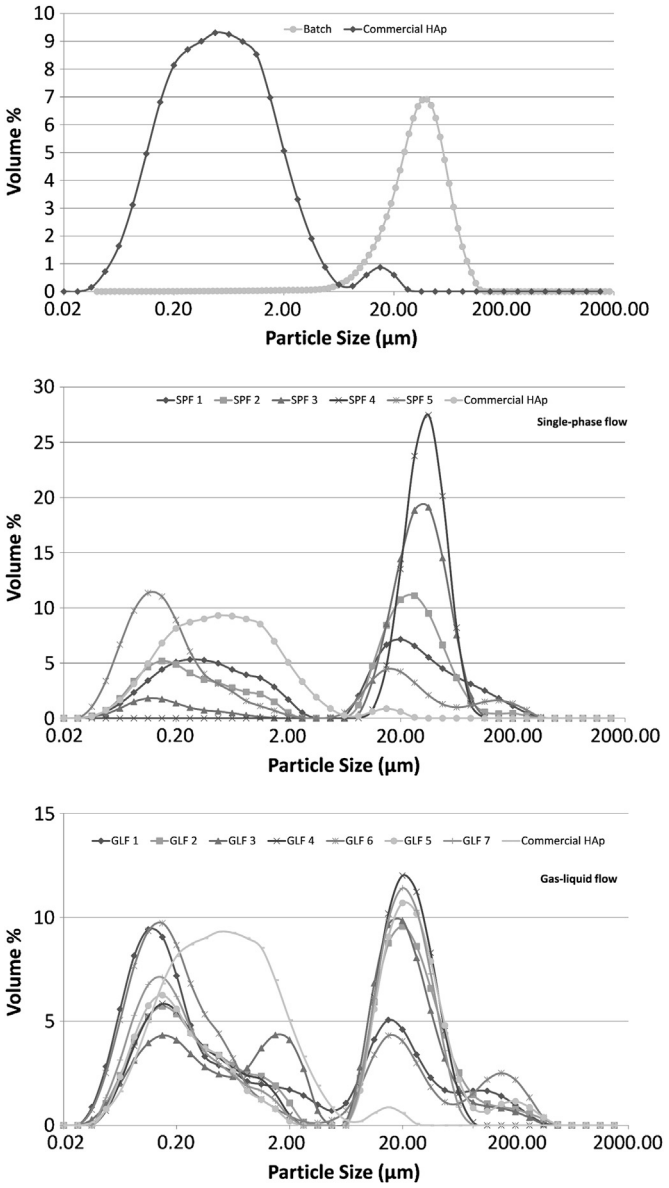

Fig. 9. Particle size distribution of the particles produced in the different reactors studied.

4. Conclusion

HAp nanoparticles were successfully prepared in an ultrasonic tubular microreactor, both in SPF and GLF configurations. Moreover, the as-prepared particles were obtained under near-physiological conditions of pH and temperature, which can be particularly relevant for bone substitution application. The effect of operating conditions on the particles properties was investigated. It was found that the particle size and the aggregation degree are affected by the liquid flow rate in the case of the SPF configuration and that the introduction of gas reduces particle aggregation and decreases the size of primary particles, especially for the higher liquid flow rates studied. Further, the obtained products show improved quality compared to commercial powder or powder produced in the stirred tank batch reactor. Primary particles are smaller, particle shape is more homogeneous, crystallinity is higher, and the aggregation degree of the particles is reduced as well as carbonate contamination. Finally, we believe that even if the reactor studied in this work does not represent a full scale production unit, it can be a useful contribution to the development of a cost-effective platform for the continuous production of high quality HAp nanoparticles.

Acknowledgments

This work was supported by the Portuguese Foundation for Science and Technology (SFRH/BD/42992/2008) through the MIT-Portugal Program, Bioengineering Systems Focus Area. The authors are thankful to Dr. Speakman for his help with the X-ray measurements and with the interpretation of the results. S.K. acknowledges funding from the Swiss National Science Foundation (SNF).

References

Bernard, L., Freche, M., Lacout, J.L., Biscans, B., 2000. Modeling of the dissolution of calcium hydroxyde in the preparation of hydroxyapatite by neutralization. Chem. Eng. Sci. 55, 5683–5692.

Castro, F., Ferreira, A., Rocha, F., Vicente, A., António Teixeira, J., 2012. Characterization of intermediate stages in the precipitation of hydroxyapatite at 37 °C. Chem. Eng. Sci. 77, 150–156.

Chen, J., Zheng, C., Gant Ang, C., 1996. Interaction of macro- and micromixing on particle size distribution in reactive precipitation. Chem. Eng. Sci. 51, 1957–1966.

Elliot, J.C., 1994. Structure and Chemistry of the Apatites and Other Calcium Orthophosphates. Elsevier, New York.

Gunther, A., Jensen, K.F., 2006. Multiphase microfluidics: from flow characteristics to chemical and materials synthesis. Lab Chip 6, 1487–1503.

Hartman, R.L., Jensen, K.F., 2009. Microchemical systems for continuous-flow synthesis. Lab Chip 9, 2495–2507.

He, Q.J., Huang, Z.L., 2007. Controlled growth and kinetics of porous hydroxyapatite spheres by a template-directed method. J. Cryst. Growth 300, 460–466.

He, Y., Wan, J., Tokunaga, T., 2008. Kinetic stability of hematite nanoparticles: the effect of particle sizes. J. Nanopart. Res. 10, 321–332.

Hung, L.-H., Lee, A.P., 2007. Microfluidic devices for the synthesis of nanoparticles and biomaterials. J. Med. Biol. Eng. 27, 1–6.

Jähnisch, K., Hessel, V., Löwe, H., Baerns, M., 2004. Chemistry in microstructured reactors. Angew. Chem. Int. Ed. 43, 406–446.

Johannsen, K., Rademacher, S., 1999. Modelling the kinetics of calcium hydroxide dissolution in water. Acta hydrochimica et hydrobiologica. 27, 72–78.

Jones, A., Rigopoulos, S., Zauner, R., 2005. Crystallization and precipitation engineering. Comput. Chem. Eng. 29, 1159–1166.

Kawase, M., Miura, K., 2007. Fine particle synthesis by continuous precipitation using a tubular reactor. Adv. Powder Technol. 18, 725–738.

Kockmann, N., Kastner, J., Woias, P., 2008. Reactive particle precipitation in liquid microchannel flow. Chem. Eng. J. 135, S110–S116.

Koutsopoulos, S., 2002. Synthesis and characterization of hydroxyapatite crystals: a review study on the analytical methods. J. Biomed. Mater. Res. 62, 600–612.

Kuhn, S., Noel, T., Gu, L., Heider, P.L., Jensen, K.F., 2011. A Teflon microreactor with integrated piezoelectric actuator to handle solid forming reactions. Lab Chip 11, 2488–2492.

Kumta, P.N., Sfeir, C., Lee, D.-H., Olton, D., Choi, D., 2005. Nanostructured calcium phosphates for biomedical applications: novel synthesis and characterization. Acta Biomater. 1, 65–83.

Landi, E., Celotti, G., Logroscino, G., Tampieri, A., 2003. Carbonated hydroxyapatite as bone substitute. J. Eur. Ceram. Soc. 23, 2931–2937.

Liu, C., Huang, Y., Shen, W., Cui, J., 2001. Kinetics of hydroxyapatite precipitation at pH 10 to 11. Biomaterials 22, 301–306.

Luque de Castro, M.D., Priego-Capote, F., 2007. Ultrasound-assisted crystallization (sonocrystallization). Ultrason. Sonochemistry 14, 717–724.

Mason, W.P., 1964. Physical Acoustics: Principles and Methods. Academic Press, New York.

Mersmann, A., 1999. Crystallization and precipitation. Chem. Eng. Process. 38, 345–353.

Osaka, A., Miura, Y., Takeuchi, K., Asada, M., Takahashi, K., 1991. Calcium apatite prepared from calcium hydroxide and orthophosphoric acid. J. Mater. Sci.: Mater. Med. 2, 51–55.

Siddharthan, A., Seshadri, S.K., Sampath Kumar, T.S., 2005. Rapid synthesis of calcium deficient hydroxyapatite nanoparticles by microwave irradiation. Trends Biomater. Artif. Organs 18, 110–113.

Song, Y., Hormes, J., Kumar, C.S.S.R., 2008. Microfluidic synthesis of nanomaterials. Small 4, 698–711.

Trippa, G., Jachuck, R.J.J., 2003. Process intensification: precipitation of calcium carbonate using narrow channel reactors. Chem. Eng. Res. Des. 81, 766–772.

Victoria, E.C., Gnanam, F.D., 2002. Synthesis and characterization of biphasic calcium phosphate. Trends Biomater. Artif. Organs 16, 12–14.

Wang, K., Wang, Y.J., Chen, G.G., Luo, G.S., Wang, J.D., 2007. Enhancement of mixing and mass transfer performance with a microstructure minireactor for controllable preparation of $CaCO_3$ nanoparticles. Ind. Eng. Chem. Res. 46, 6092–6098.

Wang, Q.-A., Wang, J.-X., Yu, W., Shao, L., Chen, G.-Z., Chen, J.-F., 2009. Investigation of micromixing efficiency in a novel high-throughput microporous tube-in-tube microchannel reactor. Ind. Eng. Chem. Res. 48, 5004–5009.

Yang, Q., Wang, J.-X., Shao, L., Wang, Q.-A., Guo, F., Chen, J.-F., Gu, L., An, Y.-T., 2009. High throughput methodology for continuous preparation of hydroxyapatite nanoparticles in a microporous tube-in-tube microchannel reactor. Ind. Eng. Chem. Res. 49, 140–147.

Ying, Y., Chen, G., Zhao, Y., Li, S., Yuan, Q., 2008. A high throughput methodology for continuous preparation of monodispersed nanocrystals in microfluidic reactors. Chem. Eng. J. 135, 209–215.

Zhao, C.-X., He, L., Qiao, S.Z., Middelberg, A.P.J., 2011. Nanoparticle synthesis in microreactors. Chem. Eng. Sci. 66, 1463–1479.

Zhou, W., Wang, M., Cheung, W., Guo, B., Jia, D., 2008. Synthesis of carbonated hydroxyapatite nanospheres through nanoemulsion. J. Mater. Sci.: Mater. Med. 19, 103–110.